2023 S.T.Yau High School Science Award (Asia)

Research Report

The Team

Name of Team Member: Shengjie Xu
School: Shanghai Foreign Language School Affiliated to SISU
Province: Shanghai
Country: China

Name of Supervisory Teacher 1: Qixiang Li
Job title: Senior high school chemistry teacher
School: Shanghai Foreign Language School Affiliated to SISU
Province: Shanghai
Country: China

Name of Supervisory Teacher 2: Wei-Hong Zhu
Job title: Professor
School: East China University of Science and Technology
Province: Shanghai
Country: China

Title of Research Report

Light-driven adaptive camouflage structures based on photoprogrammable printing ink

Date

15 September 2023

Light-driven adaptive camouflage structures based on photoprogrammable printing ink

Shengjie Xu

Shanghai Foreign Language School Affiliated to SISU, Shanghai 200083, China

Abstract

The remarkable structural colors found in animals have always captivated humans, inspiring the exploration of intricate optical phenomena by similar superstructure such as liquid crystal (LC). In LC, the incorporation of photoswitches with light-induced chirality has enabled the creation of helical structures that selectively reflect circularly polarized light. Among these photoswitches, diarylethene (DAE) has attracted accumulated attention due to its excellent thermal stability and robust fatigue resistance. However, LC need the inclusion of viscous substances to ensure stable coating onto flexible substrates owing to its fluidity. Unfortunately, this can restrict the range of structural colors, limiting their practical applications. Therefore, the primary challenge lies in striking a balance between stability and expanding the spectrum of reflected colors in the development of a highly versatile LC system. This research endeavors to enhance the LC system by optimizing the mix proportion of photoswitch, LC and polymer ink, while also exploring the potential future applications and opportunities in adaptive camouflage structures.

Keywords

Photochromic, Self-adaptive, Liquid crystal, Diarylethene, Chirality

Table of Contents

1. Introduction

Color serves as a universal language of expression, infusing the world with beauty, emotion, and distinction. Generally, natural colors can be categorized into two main types: pigment colors and structural colors. Pigment color results from the selective absorption of light by chemical chromophores, while structural color arises from the interaction between light and micro-nanostructures. Compared to pigment colors, structural color possesses distinct advantages such as fade-resistance, high resolution, and eco-friendliness.[1] In the nature, structural color is prevalent among both animals and plants. For instance, some beetle species exhibit fascinating iridescence, thanks to the well-organized arrangement of biopolymers. These structural colors serve essential purposes, including concealment, camouflage, and confusing natural predators (**Figure 1.1**).[2]

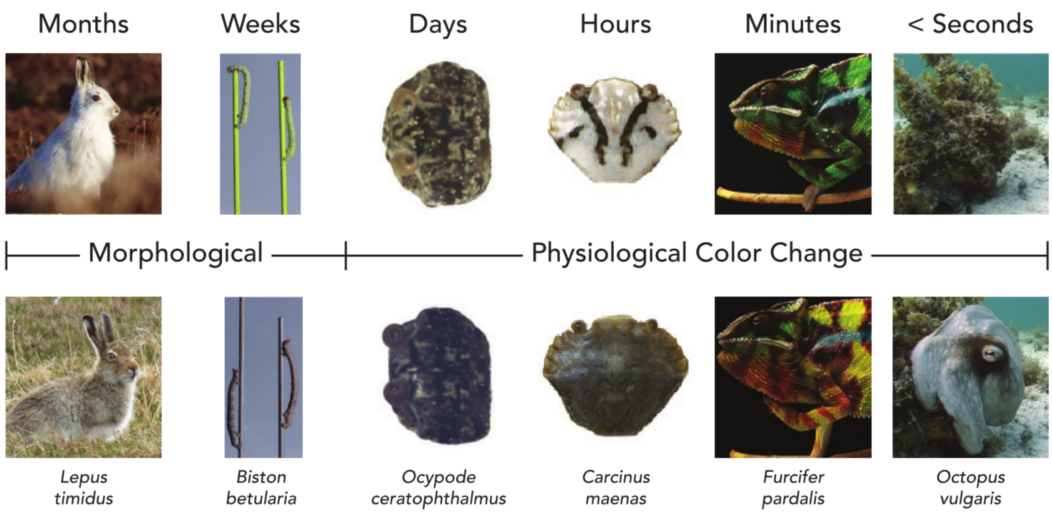

Figure 1.1 Adaptive color change with different timescales.[2]

Inspired by the structural color observed in the biological realm, researchers are currently exploring these intriguing structures, seeking to unravel their mysteries and create their potential applications. Fundamentally, the primary systems responsible for generating vivid structural color include metasurfaces and liquid crystal (LC). Compared to metasurface structures, LC offers a simpler fabrication process, lower production costs, higher efficiency, and dynamic tunability, making it a cost-effective and versatile choice for constructing structural color.[3]

As a novel phase transition between liquid and solid, LC combines the anisotropy of solids with the fluidity of liquids. Cholesteric LC (CLC) is great optical functional material because it has a spontaneous helical structure that possesses remarkable optical activity like one-dimensional photonic crystal. Generally, CLC, also known as chiral nematic LC, can be obtained by introducing chiral molecules into the nematic phase (**Figure 1.2**).[4] Due to its helical structure, CLC selectively reflect circularly polarized light (CPL). According to Bragg's law $\lambda = n\,P$[5] (λ represents the wavelength of reflected light; P represents the pitch of the helical structure; n represents the average refractive index of the LC system), the wavelength λ is proportional to the pitch P when the LC is determined (i.e. n remains unchanged). When the pitch of the CLC matches the wavelength of visible light, it selectively reflects light of specific wavelength, enabling the achievement of various colors in displays. To more effectively characterize the capacity of chiral molecules in causing nematic distortion to generate helical structures, the helical twist power (HTP) is frequently quantified using the equation $\beta = 1 / (c\,P)$, where c denotes the concentration of chiral molecules. Typically, the HTP is evaluated through the Grandjean-Cano method.[6]

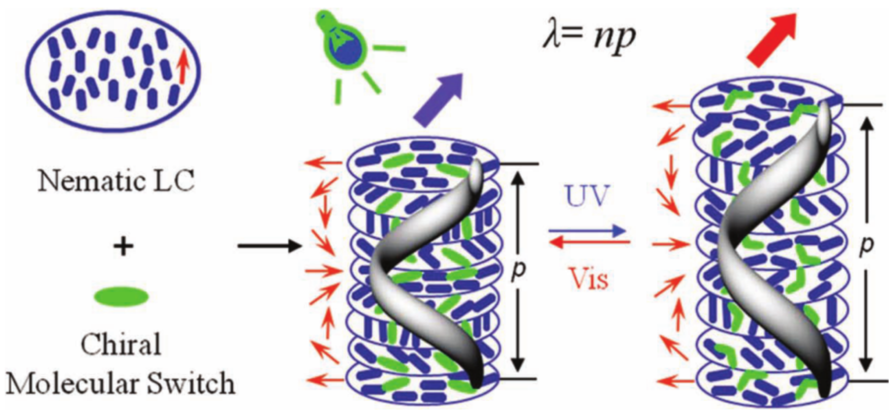

Figure 1.2 Illustration of light reversibly modulated the helical pitch of CLC.[4]

Since the discovery of CLC, modulating its helical pitch by external stimuli has been a major research focus because it enables continuous reflected wavelength in a wide range and constructs a series of structural colors. Compared with other stimuli like electric, magnetic, and temperature, light performs unique advantages of remote, non-invasive, temporal, and spatial manipulation.[7] Here, chiral photoswitches exhibit different features (**Figure 1.3**).[8] Azobenzene and spiropyrane are sensitive to heat, which show poor thermal stability. Fulgide always generate multiple products, which show poor fatigue resistance. Therefore, DAE has become our preferred photoswitch due to its excellent thermal stability and fatigue resistance.[9]

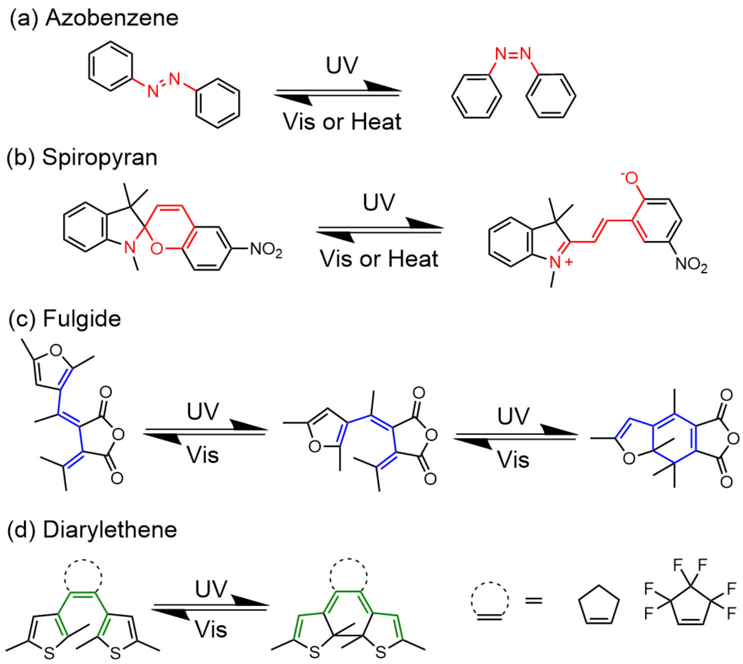

Figure 1.3 Chemical structures of photoswitches. (a) azobenzene, (b) spiropyran, (c) fulgide, (d) diarylethene.

However, due to the rapid rotation of the aromatic group in the side chain of the DAE photoswitch, its chiral isomers cannot be separated, further limiting its responsiveness to chiral signals. Here, a new type of sterically hindered ethene bridge is proposed for the first time, which allows multiple-digital manipulation of soft LC-based systems with excellent thermal stability and robust fatigue resistance.[10] This unique CLC shows excellent modulation performance with a wide range of modulation. However, CLC has a severe problem—high fluidity, which restricts it to be sealed in a close system such as layers of glass. The high fluidity makes it challenging to coat onto corresponding flexible substrates, resulting in poor universality and thus limiting the application. To increase viscosity, the current approach mainly involves photopolymerization, but this method often significantly increases the viscosity of the LC system, greatly reducing its inherent manipulable range, limiting the result of the light-driven change. Therefore, finding a balance between modulation and flexibility is a significant challenge in the development of dynamic broad-range flexible optical devices. Our approach is to balance the two properties by regulating the mix proportion of the photoswitch—DAE, the liquid crystal—TEB300 and polymer ink.

2. Results and Discussions

2.1 Photoprogramming of printing ink with suitable viscosity and broad-range structure color

Owing to high fluidity, CLC cannot be applied to some textures because they will easily flow and cannot be restricted in pre-designed region. In order to achieve suitable viscosity in LC system, some viscous substances need to be added. At the same time, a wide range of reflection colors of the chiral CLC needs to be ensured. Therefore, the viscous substances should be investigated to find the best proportion for the broad-range modulation. The first step is to prepare photoprogrammable printing ink of CLC using TEB300 and the chiral photoswitch DAE.

As mentioned in the introduction, DAE is chosen in this study not only due to the excellent thermal stability, but also the robust fatigue resistance, which ensures the stability and lifetime of devices based on light-driven structure. By analyzing the structure of DAE, we find that due to the free rotation of the side chain, the open form can be divided into parallel isomers and antiparallel isomers. According to the Woodward-Hoffman rule, only antiparallel isomers can undergo photocyclization reactions under light, exhibiting photoactivity. In addition, parallel isomers do not possess chirality due to their symmetric structure, while antiparallel isomers have a pair of axial chirality isomers, namely *P* helix and *M* helix. Under illumination, they will generate a pair of corresponding central chirality isomers, namely (*R*,*R*) and (*S*,*S*). To regulate the chirality of DAE, one can modify the side chain of chiral groups or limit the rotation of side chain by steric hindrance effect, which are referred to as extrinsic and intrinsic chirality respectively. When the UV light is applied to DAE, the structure of DAE changes from the open state (left) to closed state (right) with change from *M* helix to chiral center (*S*,*S*); when the visible light is applied, the structure of DAE changes back reversibility (**Figure 2.1 B**).

Since the chirality of DAE changes as UV light is applied, the helical pitch of the LC system changes as well and causes the reflection color change. As show in **Figure 2.1 C**, the structure of the chiral DAE gradually changes as applying the UV light, the helical pitch changes accordingly from small to large. The change of helical pitch, according to Bragg's law $\lambda = n\ P$, results in the change of the reflection wavelength. Therefore, the reflection color we observe changes from blue to green and to red.

To achieve photoprogramming of printing ink with a suitable viscosity and a broad-range structure color, we mix some viscous substance (**Figure 2.1 D**) (used in ink, coatings, adhesives, pharmaceuticals, cosmetics, food, fillers, adhesives, etc.) with the LC system. After a mixture of viscous substances and LC is made, it can be applied to a substrate so that patterns can be painted on flexible material to observe the phenomenon of light-driven reflection colors.

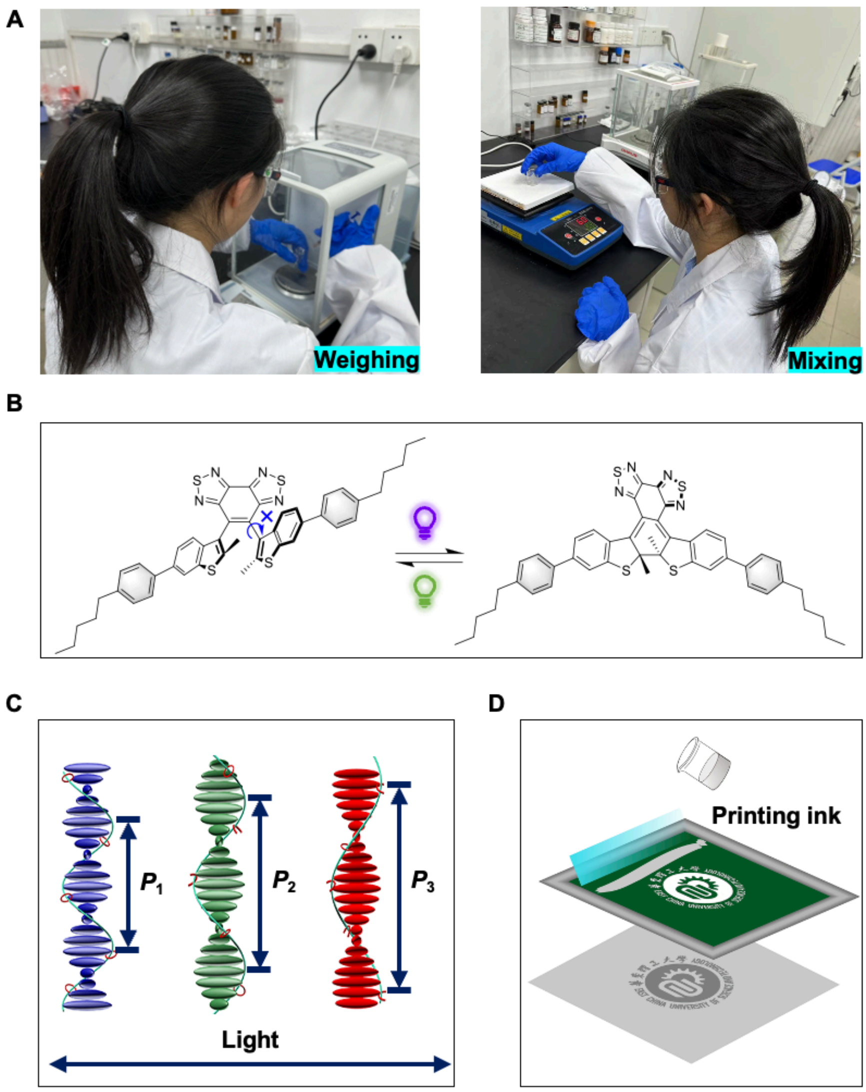

Figure 2.1 Photoprogramming of printing ink with suitable viscosity and broad-range structure color. (A) The researcher is weighing and mixing the substances. (B) The structural change of DAE under UV light and visible light. (C) The change of the helical pitch in the LC system under UV light irradiation. (D) Printing ink is added to the LC system so that patterns can be painted on a flexible substrate.

2.2 Exploring the optimal mix proportion of photoswitch, liquid crystal and polymer ink

The process in 2.1 was repeated several times to make up a range of different proportions of polymer ink and LC.

First, we would like to explore the proportion of the chiral photoswitch at which the LC system can reach the broad-range reflection color. To begin with, we test a system of 2.0 wt% DAE (**Figure 2.2 A**). The system does not reflect any visible light, which makes the pictures seeming black. This is probably because the weighted percentage of DAE is too low in the system so that the system does not contain enough molecules that change their structures to create helical pitch large enough to exhibit reflection colors within the visible light range. Then we choose to test a system of higher weighted percentage of DAE, hoping to figure out the highest weighted percentage that can exhibit reflection colors within the visible light range. 4.2 wt% of DAE is tested and the results are shown is **Figure 2.2 B**. The first two pictures, taken at the early state of the system under UV light, appear black as well, suggesting that the system contain too much molecules that change their structures so that the helical pitch of the system is too large to exhibit reflection colors within the visible light range. Although the final picture in **Figure 2.2 B** exhibits green color, the reflection color range has not been optimal. The next test is a system of 3.4 wt% DAE (**Figure 2.2 C**). The reflection color range of this system is green to red, which is nearer to the optimal proportion but still not the perfect one. After that, we test 3.8 wt% DAE (**Figure 2.2 D**), whose reflection color range is from blue to red, which is the optimal range. Therefore, the best proportion of DAE is 3.8 wt% in LC as it exhibits the broad-range reflection color.

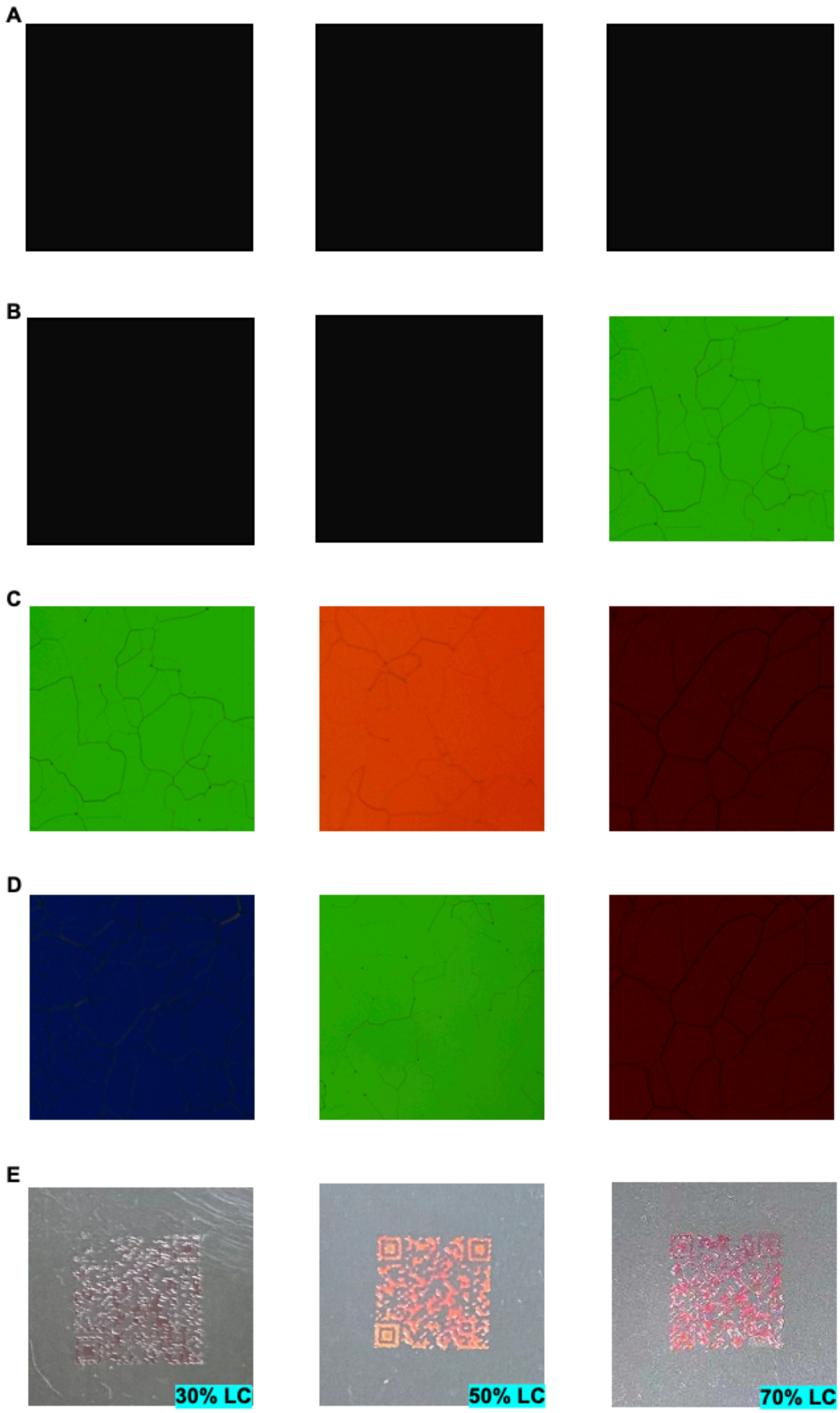

Figure 2.2 Exploring the optimal mix proportion of photoswitch, liquid crystal and Polymer ink. (A) 2.0 wt% of DAE in system showing reflection color range from green to red. (B) 4.2 wt% of DAE in system showing reflection color range from green to red. (C) 3.4 wt% of DAE in system showing reflection color range from green to red. (D) 3.8 wt% of DAE in system showing reflection color range from blue to red. (C) The three systems with different proportion of LC tested.

As mentioned in 2.1, certain viscous materials need to be added in the LC system to achieve stable pattern on substrates. When the viscosity of the system increases, less printing ink can penetrate the silk-screen so that the patterns will be discontinuous. However, when the liquidity of the system is too high, more printing ink than needed penetrate the substrate so that the patterns will be hazy. When there is 30% of LC in the system, not enough printing ink can penetrate the substrate so that the QR code is discontinuous. When there is 70% of LC in the system, the details and edges of the QR code are obscure. The 50% LC system exhibits the optimal pattern with clear edges and details. Therefore, the optimal proportion of LC in the system is 50% (**Figure 2.2 C**).

2.3 Testing the optical performance of the photoprogrammable printing ink

Here, we test the reflection color range, the ability to apply on different substrates, the thermal stability and fatigue resistance.

First, we test the reflection color range by printing the liquid crystal system on the substrate and applying UV light and visible light (**Figure 2.3 A**). We applied the UV light for different time and the structural color of LC system changes accordingly (**Figure 2.3 B**): blue (0 s), green (6 s), yellow (13 s) and red (25 s). Then the visible light is applied and the LC system changes back reversibly: red (0 s), yellow (14 s), green (27 s) and blue (45 s). Therefore, the wide reflection color range from blue to red is guaranteed.

Then we test the ability of the LC system to apply on different substrates. Another four substrates that we use: glass, PET, paper and wood (**Figure 2.3 C**). All the patterns in the four substrates are clear with sharp edges. Although there is a slight difference in color on these four substrates (on the paper and wood, the color is slightly darker), the distinct edges of each pattern clearly verify the generality to apply on different substrates and even flexible substrates of the system, which is a merit of our system.

The next property that we test is the stability of the color and the pattern. As **Figure 2.3 D** shows, the red pattern like a smart phone remains the same color with sharp edges in at least 24 hours, without any dispersion, which guarantees the high stability and future application in anti-counterfeiting and adaptive camouflage.

The final testing is to test a fatigue resistance of the system. Fatigue resistance is the stability of the system (color) after constant switch from UV light to visible light for many times. The red and blue colors that the system exhibits during 20 continuous switches, thereby providing excellent lifetime of photonic structures (**Figure 2.3 E**).

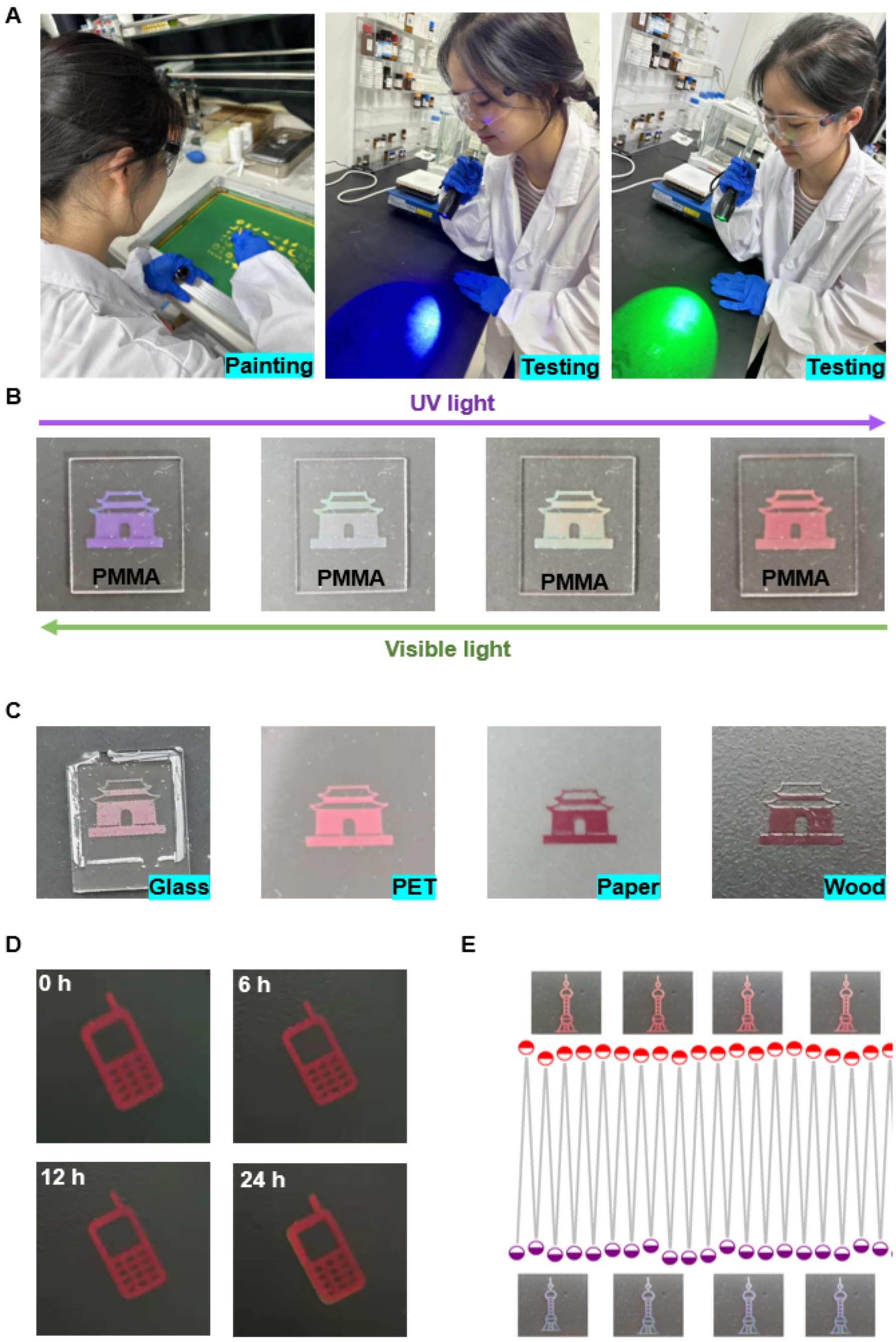

Figure 2.3 Testing the optical performance of the photoprogrammable printing ink. (A) Printing the liquid crystal system on the substrate and applying UV light and visible light. (B) We applied the UV light (365 nm; 4 mW cm^{-2}) for different time and the LC system changes accordingly: blue (0 s), green (6 s), yellow (13 s) and red (25 s). Then the visible light (530 nm; 1 mW cm^{-2}) is applied and the LC system changes back: red (0 s), yellow (14 s), green (27 s) and blue (45 s). Therefore, the wide reflection color range from blue to red is guaranteed. (C) All the patterns in the four substrates (glass, PET, paper and wood) are clear with sharp edges. (D) The red pattern remains with clear edges in 24 hours. (E) The red and purple colors that the system exhibits during 20 continuous switches between UV light and visible light.

2.4 Manipulating optical microstructures with broad-range structure color

After the macroscopical performance of the system is tested, we move on to test the macroscopical optical performance of the system. Here, we test two optical performances in total, texture and spectrum.

The LC samples were observed using a polarized optical microscope (ILVPOL 100, Nikon) with crossed polarizers under reflection mode and the optical textures were recorded using a charge-coupled device (CCD) camera. We first focus the microscope to display a clear picture of the sample and then observe the samples (**Figure 2.4 A**). A fiber-coupled spectrometer (Avaspec-ULS2048, resolution: 2.0 nm, 200-1100 nm) was used to detect the reflection spectra from the sample.

To further verify the optical performance, a patterned image was recorded in the light-driven LC sample using silk-screen printing, showing the emergence of a well-defined blue pattern after UV irradiation for 0 s, which was followed by the successive color change to green (5 s), yellow (13 s) and red (25 s) with sustained UV exposure (**Figure 2.4 B**). Remarkably, no obvious color movement of boundaries with the removal of an illumination stimulus while images at any transitional state remained unaltered in blue, green and red. This result exhibits the multi-stable characteristic, as well as fast responsive behavior and precise patterning, so that optical digital programming, the selection and extraction of any preferred color image as well as reflection spectra via non-invasive light stimulation is enabled.

In particular, the binary color is capable of generating absorbance or transmittance difference in the reflected light, depending upon the wavelength located at the reflection band of LC systems, thereby creating an illumination diffractive effect. To demonstrate this, a 633 nm helium-neon (He-Ne) laser, which was insensitive to the photoswitch DAE, was converted to a CPL probe beam to detect the diffraction of red-and-dark micropatterns (**Figure 2.4 C**). The most distinctive and strong diffraction patterns, such as the one-dimensional and two-dimensional gratings, which confirmed the micropattern regularity. With diffraction observed, it is proven that the microstructure of the system is well designed, which further demonstrates the high quality of the patterns that this system can print.

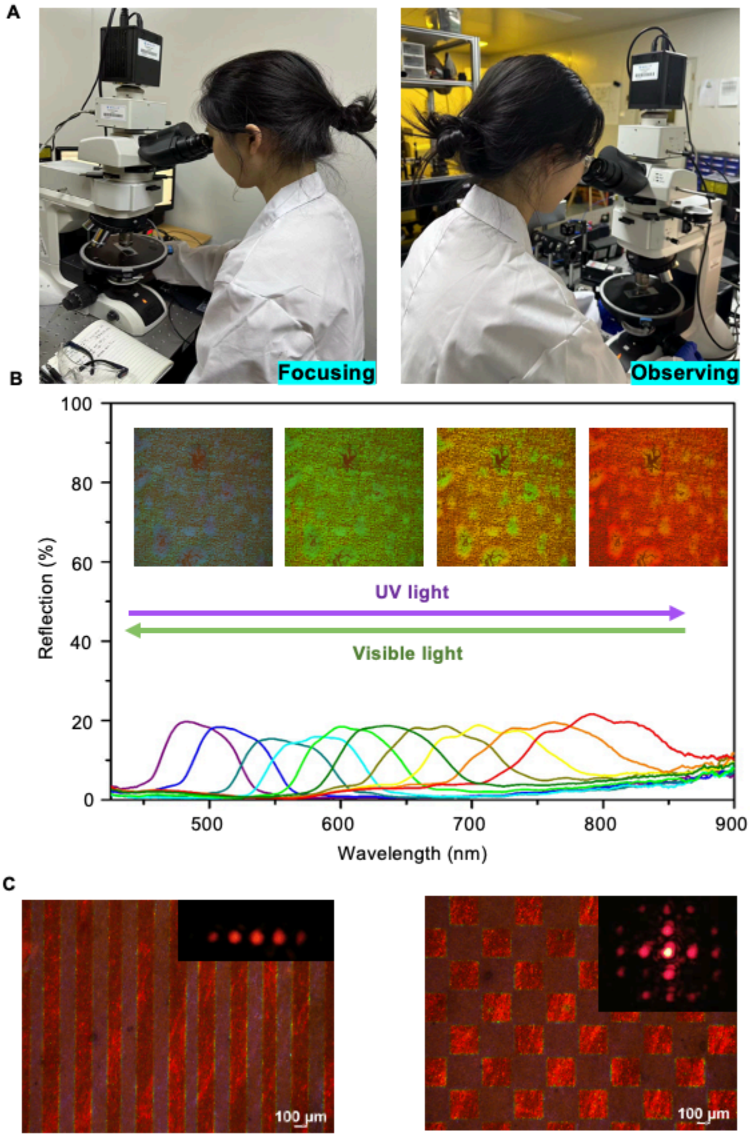

Figure 2.4 Manipulating optical microstructures with broad-range structure color. (A) Focusing the polarized optical microscope and observing the structures. (B) The spectrum of the photoprogrammable printing ink under UV light and visible light. (C) The microstructure textures of one-dimensional and two-dimensional gratings and the corresponding diffraction spots.

2.5 Achieving application of adaptive camouflage structures

After testing the performance of the system, we explore the future applications of the system on flexible substrates.

Mastering methods to control adaptive materials holds significant importance in many industrial and technological fields. Besides the common application of camouflage, in the medical field, materials capable of adapting to the body's environment can precisely achieve drug delivery. For architecture, materials that adapt to the environment can truly provide comfort throughout the seasons. Additionally, in optical, chemical, and other experimental sciences, materials that can adapt to the environment also play a crucial role.

Materials capable of changing color play an increasingly important role in various fields. The most obvious uses of adaptive material, which can automatically adjust their color and texture to the environment around them, are camouflaging and concealment. This technology has applications in areas such as the military, hunting and conservation of wildlife. The use of color adaptive material which can be adapted to various lighting conditions is also possible for the purposes of creating security signs and road markings that increase visibility. Beyond responding to external colors, certain materials can change color based on temperature variations, providing interesting solutions for temperature monitoring. Even in education, these materials can help students visualize changes in properties like temperature and acidity, making it easier to grasp knowledge. In the realm of art, utilizing color-changing materials to create creative works and installations can captivate audiences and express ideas with greater impact.

In this study, we use leaves as the substrate. As leaves change color in four seasons accordingly, from green or yellow to red or brown, we are able to test the self-adaptive photochromic performance of the system as well. The **Figure 2.5** shows that the refined system can change color and camouflage according to the environment and the light-driven control is highly effective. In the case of architecture, materials that adapt to the environment can provide comfort throughout the year. Additionally, in optical, chemical, and other experimental sciences, materials that can adapt to the environment also play a crucial role.

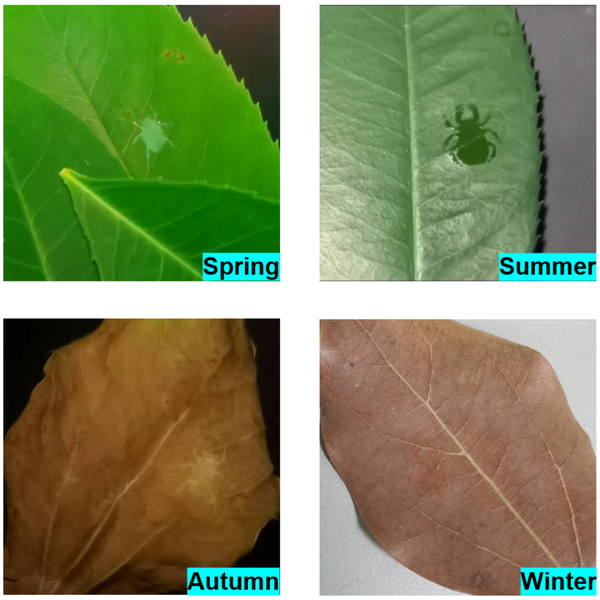

Figure 2.5 Achieving application of adaptive camouflage structures. Exploring the optimal mix proportion of photoswitch, liquid crystal and polymer ink. A series of leaves in different colors are used to simulate the situations in different seasons. In all cases our system can camouflage well according to the environment.

3. Conclusions

Based on this study, we reach the following conclusions: 1) we successfully achieve both wide reflection color range and appropriate viscosity in the photochromic LC system. The appropriate proportion of the viscous substance and the LC system is 1:1. 2) We examine the oily texture and the spectrum of the material so that we make sure that the material is well-performing with broad-range structure color. 3) We discuss the potential application of this material into anti-counterfeiting and onto flexible substrates such as leaves, which paves a promising avenue toward adaptive camouflage materials.

4. Experimental Section

4.1 Constructing printing ink with suitable viscosity and broad-range structure color

The procedure to prepare a system of liquid crystal and chiral molecules is shown in **Figure 4.1 A**. The first step is to tare the bottle weight and weigh the liquid crystal (in this case TEB300) with bottle while adding it into the bottle. For example, the weight of the LC is 33 mg. We first try with the mass proportion of 2.0 wt% for DAE. According to the calculation, the mass of DAE needed is 0.67 mg. Then, we weigh DAE as calculated and mix it with the LC system. The next part is to heat and stir the LC system prepared using the magnetic stirrer to let DAE fully dissolve in the liquid crystal. During this process, we constantly move the bottle in a circle to let the small magnetic stirrer to spin in every corner of the system so that DAE can be fully dissolved. The polymer printing ink is added in the system as well to increase the viscosity.

The next step is to print the prepared system on the silk-printing substrate and the house-pattern on the paper is created. To test if this sample has all kinds of proper properties, it is irradiated by UV light and visible light. The results shows that this proportion is not the appropriate one since it only exhibits the black color. We further test other proportions: 4.2 wt%, which exhibits only the black color and the green color. Further tests are 3.4 wt% and 3.8 wt% respectively. The tests show that 3.4 wt% of DAE can exhibit colors from green to red, while 3.8 wt% of DAE can exhibit colors from blue to red.

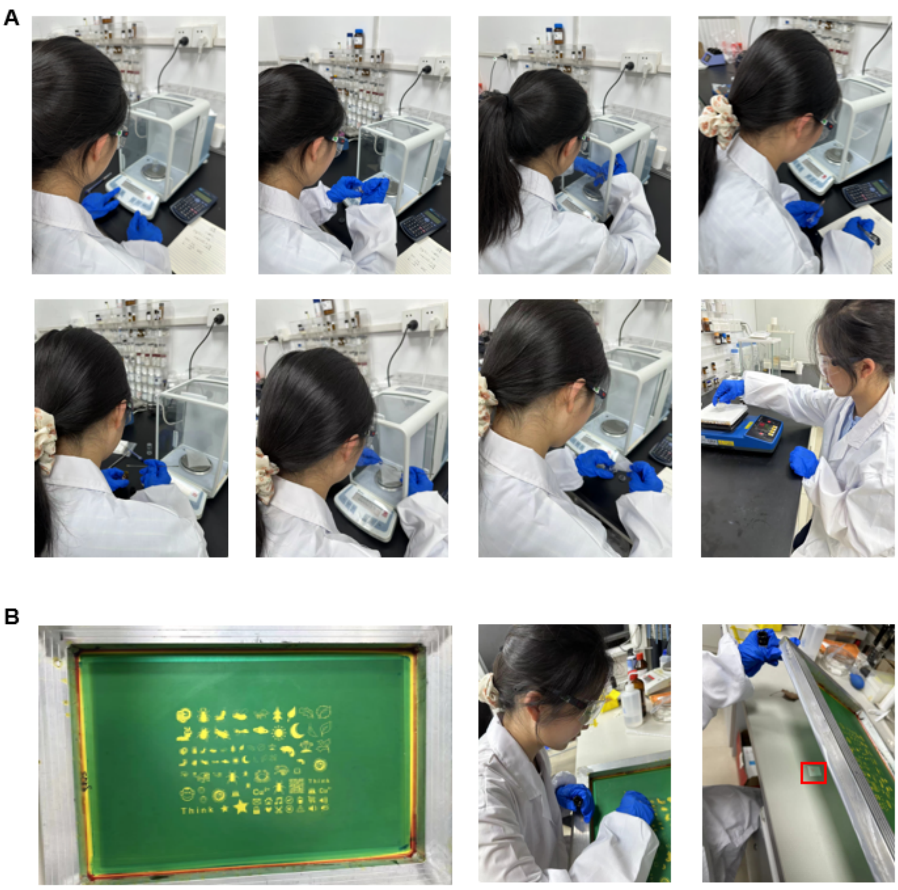

Figure 4.1 Constructing printing ink with suitable viscosity and broad-range structure color. (A) (From left to right, top to bottom) Taring the weight of the bottle; Taking some amount of TEB300 out; Adding TEB300 while weighing the system; Calculating the mass of DAE needed; Taring the weighing paper; Weighing DAE on the weighing paper; Stirring the system using the magnetic stirrer. (B) (From left to right) The silk-screen printing substrate used to print patterns; Printing the LC system on the substrate; The house-like pattern printed on the white paper through the substrate.

4.2 Testing the optical performance: texture and spectrum

To achieve wavelength modulation, all the LC samples were irradiated via a 530 nm collimated LED light source (M530L3, Thorlabs) or a 365 nm UV LED source (SunSpot 2, Uvitron). To observe the LC samples, polarized optical microscopy (POM, Nikon LVPOL 100) was used under reflection mode, the charge-coupled device (CCD) camera was used to record optical textures, and the fiber coupled spectrometer (Avaspec-ULS2048, resolution: ~2.0 nm, 200-1100 nm) was used to collect the reflection spectra from the sample. The software CapStudio is used for observing the optical textures and AvaTex is used for collecting the reflection spectra.

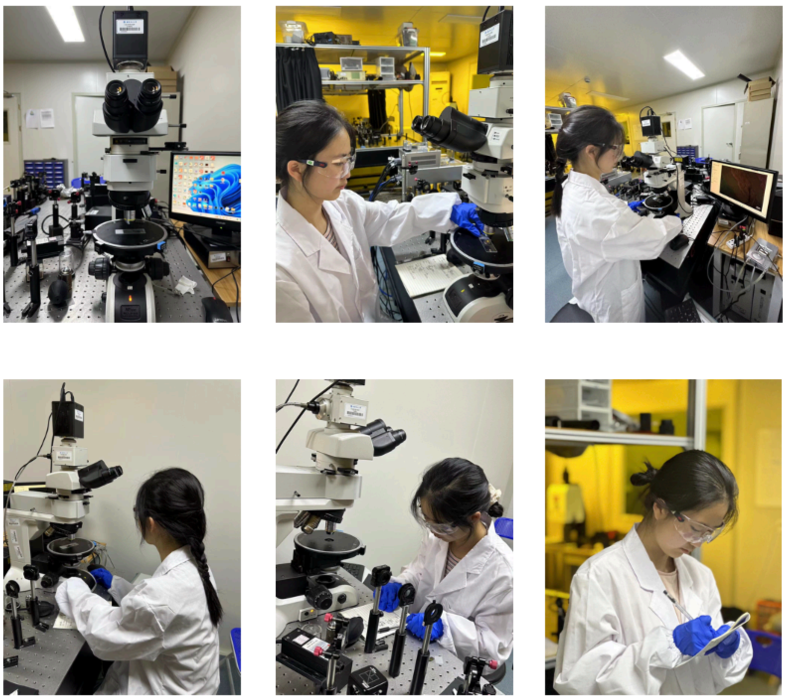

Figure 4.2 Testing the optical performance: texture and spectrum. From left to right, top to bottom: Polarized optical microscopy; Placing the sample; focusing; observing; recording the results.

4.3 Designing application of adaptive camouflage structures

After testing all the properties, we turn our sight to the application of the sample on flexible substrates. Leaves are great examples for developing an adaptive camouflage structure. Therefore, we use the silk-screen printing substrate to print the sample on the leaves. As Figure 4.3 demonstrates, the bug-like pattern can adapt to the environment and has perfect camouflage effect.

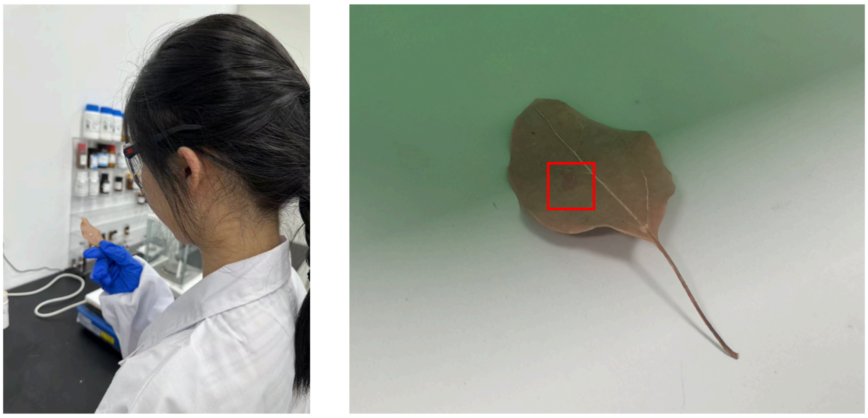

Figure 4.3 Designing application of adaptive camouflage structures. Leaves are great examples for developing an adaptive camouflage structure, and the bug-like pattern can adapt to the environment and has perfect camouflage effect.

5. Acknowledgement

The author would like to thank Professor Wei-Hong Zhu and his research team for their help in the experiment. Under the guidance of Professor Wei-Hong Zhu and the help of Dr. Honglong Hu, the author Shengjie Xu independently completed all the experiments in this thesis. I hereby sincerely thank all of the people who contributed to this research project and paper.

6. References

1 盛善祥,吴蒙,宋霄,支超,孟家光,刘亚明. 高饱和度、高稳定性光子晶体结构色织物的研究进展[J]. *印染*, **2023**, *49*, 74-81.

2 Wilson, D. J., Lin, Z., Bower, D. Q. & Deravi, L. F. Engineering color, pattern, and texture: From nature to materials. *Matter*, **2021**, *4*, 2163-2171.

3 Bisoyi, H. K. & Li, Q. Liquid crystals: Versatile self-organized smart soft materials. *Chem. Rev.*, **2022**, *122*, 4887-4926.

4 Wang, Y. & Li, Q. Light-driven chiral molecular switches or motors in liquid crystals. *Adv. Mater.*, **2012**, *24*, 1926-1945.

5 Pieraccini, S., Masiero, S., Ferrarini, A. & Piero Spada, G. Chirality transfer across length-scales in nematic liquid crystals: Fundamentals and applications. *Chem. Soc. Rev.*, **2011**, *40*, 258-271.

6 Heppke, G. & Oestreicher, F. Notizen: Bestimmung des helixdrehsinnes cholesterischer phasen mit der grandjean-cano-methode / determination of the helical sense of cholesteric liquid crystals using the grandjean-cano method. *Z. Naturforsch.*, **1977**, *32*, 899-902.

7 刘晓珺, 秦朗, 俞燕蕾. 胆甾相液晶螺旋方向的光调控[J]. *化学进展*, **2023**, *35*, 247-262.

8 Dattler, D., Fuks, G., Heiser, J., Moulin, E., Perrot, A., Yao, X. & Giuseppone, N. Design of collective motions from synthetic molecular switches, rotors, and motors. *Chem. Rev.*, **2020**, *120*, 310-433.

9 胡宏龙, 郑致刚, 朱为宏. 基于光控二芳基乙烯的手性向列相液晶体系研究进展[J]. *化工学报*, **2022**, *73*, 3381-3393.

10 Zheng, Z., Hu, H., Zhang, Z., Liu, B., Li, M., Qu, D.-H., Tian, H., Zhu, W.-H. & Feringa, B. L. Digital photoprogramming of liquid-crystal superstructures featuring intrinsic chiral photoswitches. *Nat. Photonics*, **2022**, *16*, 226-234.